Online Supplementary Material

Suppression of Activated FOXO Transcription Factors in the Heart Prolongs Survival in a Mouse Model of Laminopathies

Gaelle Auguste, Ph.D., Priyatansh Gurha, Ph.D., Raffaella Lombardi, M.D., Ph.D., Cristian Coarfa, Ph.D.* James T. Willerson, M.D., Ali J. Marian, M.D.

Center for Cardiovascular Genetics, Institute of Molecular Medicine and Department of Medicine, University of Texas Health Sciences Center at Houston, Texas Heart Institute, and

* Baylor College of Medicine, Houston, TX 77030

Running title: Improved survival upon suppression of FOXO TFs in laminopathies

Address for Correspondence:

AJ Marian, M.D.
Center for Cardiovascular Genetics
6770 Bertner Street
Suite C900A
Houston, TX 77030
713 500 2350
Ali.J.Marian@uth.tmc.edu

METHODS

The studies conformed to the Guide for the Care and Use of Laboratory Animals published by the US National Institutes of Health and were approved by the Animal Care and Use Committee and the Biological Safety Committee of the University of Texas Health Science Center-Houston.

The data, methods used in the analysis, and materials used to conduct the research will be made available to any researcher for purposes of reproducing the results or replicating the procedure. The transcriptomic data will be deposited in NCBI GEO Profile and maintained indefinitely.

***Lmna*$^{-/-}$ and wild type (WT) littermates:** The phenotype in the *Lmna*$^{-/-}$ mice has been published. [1, 2] *Lmna*$^{-/-}$ and age- and sex-matched WT littermate mice were used as controls in these experiments, the latter as controls. Mice were maintained in the C57BL/6 background and housed in a 12-hour light/night cycle facility with *ad libidum* food and water. Genotyping was performed by polymerase chain reaction (PCR) of DNA extracted from tail-clip. Oligonucleotide primers used in PCR reactions are listed in Online Table I.

Mice were euthanized by carbon dioxide inhalation followed by cervical dislocation. Hearts were rapidly excised, rinsed twice with ice-cold Phosphate Buffered Saline (PBS), and dry-blotted before use or storage at -80 °C.

Survival: Survival was analyzed by constructing Kaplan-Meier survival plots.

Gross morphology: Mice were weighted weekly to record body weight (BW). Heart was excised from the chest, after euthanasia, and heart weight/body weight (HW/BW) ratio was calculated in age- and sex-matched littermate mice.

Echocardiography: Cardiac size and function were assessed in age- and sex-matched littermate mice by 2D, M mode, and Doppler echocardiography, as published using a Vevo 1100 ultrasound imaging system equipped with a 22-55 MHz MicroScan transducer (MS550D) (FUJIFILM VisualSonics Inc., Toronto, ON, Canada). [3-6] Echocardiography was performed in 2- and 4-week old WT and *Lmna*$^{-/-}$ littermate mice. In brief, mice were lightly anesthetized by intraperitoneal injection of sodium pentobarbital (60 mg/Kg body weight). After removing the chest fur with a hair removal cream (Nair), mice were positioned

supine on a heating pad with embedded ECG leads. ECG and respiratory rate were recorded during the study**.** Wall thicknesses and left ventricular dimensions were measured from M-mode images from the parasternal two-dimensional short-axis view at the tip of the mitral leaflet, using the leading-edge method. Left ventricular fractional shortening and mass were calculated from the measured indices. Echocardiographic data were measured in 3 cardiac cycles and mean values were used.

Isolation of adult cardiac myocytes: Mice were anesthetized by intra-peritoneal (I.P.) injection of pentobarbital (62 mg/Kg) followed by I.P. injection of heparin (200U) to prevent clot formation.[4] The heart was excised and placed in a Ca^{2+} free perfusion buffer [120 mM NaCl, 15 mM KCl, 0.6 mM KH_2PO_4, 0.6 mM Na_2HPO_4, 1.2 mM $MgSO_47H_2O$, 30 mM Taurine, 4.6 mM $NaHCO_3$, 10 mM HEPES, 10 mM 2,3-Butanedione monoxime (BDM), and 5.5 mM Glucose; pH 7.0]. The heart was cannulated through ascending aorta, the cannula was positioned above the aortic valves, and the heart was connected to a retrograde perfusion system. The heart was perfused with the perfusion buffer at a constant rate of 4 mL/min for 2 minutes, then 250 units/mL of Collagenase II (Worthington, Lakewood, NJ) was added to the buffer, and the perfusion was continued for another 2 minutes. The digestion buffer was then supplemented with 12.5 μM $CaCl_2$; the perfusion was continued until complete softening of the myocardium. The heart was then cut into small pieces in the digestion buffer, and cells were dissociated by gentle pipetting. Upon complete dissociation of the cells, calf serum (10% in final volume) was added to stop the enzymatic digestion, and cells were passed through a 100 μm nylon mesh. Myocytes were left to sediment by gravity in the presence of 2 mM ATP and pelleted by centrifugation at 20 g for 3 min. Sequential concentrations of calcium (100 μM, 400 μM, and 900 μM), were re-introduced to the cells in presence of 2 mM ATP . The final isolate was resuspended in a plating media (MEM media, 1% penicillin-streptomyocin, 10% Calf serum, 10 mM BDM, and 2 mM ATP) and placed on laminin-coated cover glasses in a 2% $_2$ incubator at 37 °C or were immediately frozen.

Isolation of neonatal mouse ventricular myocytes: Hearts from 1- to 2-day old wild-type pups were rapidly excised from the chest. Atria were cut out and pooled ventricules were minsed in ice cold ADS buffer (120 mM NaCl, 5.4 mM KCl, 5.5mM Glucose, 12.5 mM NaH_2PO_4, 0.8 mM $MgSO_4$, and 20mM HEPES, pH = 7.2). Ventricular tissue was digested by successive enzymatic digestions in a buffer containing 70U/mL of Collagenase II (Worthington cat# LS004176) and 0.6mg/mL of pancreatin (Sigma # P3292) at 37 °C. Cell suspension was thereafter purified by pre-plating for 1 hour and half at 37°C, 5% CO_2. Non-adherent cells were then recovered, counted and grown on chamber slides (Corning, 08-774) coated with Poly-D-Lysine (Sigma, # A-003-E) in DMEM supplemented with 10% bovine calf-serum (Gibco, #16170078).

Cells were infected with recombinant adenoviruses expressing a constitutively active FOXO3 or vector adenoviruses (Vector Biolabs, #1025 and #1060) on day 2 at a multiplicity of infection of 20 for 48 hours. In the constitutively active form of FOXO3 ($FOXO3^{AAA}$) three phosphorylation sites (Thr^{32}, Ser^{253} and Ser^{315}) were mutated for alanine. The construct mimicks FOXO3 activation, as observed in the *Lmna*$^{-/-}$ myocytes.

To assess superoxide anion production by the mitochondria, neonatal mouse cardiac myocytes were stained with MitoSOX Red (5 μM; InvitroGen M36008) for 30min according to manufacturer's instructions. Then, cells were fixed and the nuclei were counterstained with DAPI.

Histology: Myocardial histology was examined upon staining of thin (4-5 μm) myocardial sections with Masson trichrome and Sirius Red (SR), as described. [4, 7, 8] Extent of interstitial fibrosis was quantified by determining collagen volume fraction (CVF) in at least 10 high magnification fields (x40) per section and 5 sections per heart. [7] Images were analyzed using the ImageJ software.

Immunofluorescence (IF): IF was performed as previously described. [6, 83] The detailed list of antibodies used is provided in the Supplemental Table I. Briefly, myocardial frozen section were fixed for 15 min at room temperature in 4% formaldehyde. After extensive washes, sections were blocked in 5% donkey serum with PBS-0.3% Triton X-100 for 1 hour at room temperature and then were incubated with

the primary antibodies in 1% bovine serum albumin (BSA) in PBS-0.3% Triton-X-100 at 4°C overnight. Sections were then incubated with appropriate secondary antibodies conjugated with fluorescent dyes. Nuclei were conterstained with 0.1 mg/mL of 4′, 6 Diamidino-2-phenylindole dihydrochloride (DAPI) (Sigma-Aldrich St Louis, MO; cat# D8417). Slides were mounted using fluorescent mounting medium (Dako cat# S3023). Section were then examined with an inverted fluorescent microscope (Zeiss, Axioplan Fluorescence Microscope). Image acquisition was completed with AxioVision software. Nuclear localixation of FOXO3 was determined by counting the number nuclei stained positive for FOXO3 in a minimum of 10 high magnification fields (X40), 2-3 thin sections, per heart, and 3 mice per experimental group (a mimimum of 5,000 nuclei per heart).

Junctophilin (JPH2) and α-actinin (ACTN2) staining were examined on thin frozen section showing myofibrils in the longitudinal axis. Iterative deconvolution was performed on Z-stack acquired images at a very high magnification (X100). A minimum of 5 fields, 2-3 thin sections per heart, and 3 mice per experimental group were examined.

Detection of apoptosis: Apoptosis was detected by nick-end labelling of DNA with the TUNEL assay using In Situ Cell Death Detection Kit (Roche catalogue # 11684795910 and 12156792910), per manufacturer instructions. [4, 9] In brief, formalin fixed-paraffin embedded thin myocardial sections were dewaxed before processing. Simiarly, neonatal mouse cardiac myocytes were fixed for 15 min in 4% paraformaldehyde and processed similarly. Samples were treated with Proteinase K (10 mg/ml in 10 mM Tris/HCl, pH 7.5) for 20 min at 37°C and subsequently incubated with the TUNEL reaction mixture for 1 hour at 37°C. Nuclei were counterstained with DAPI and after extensive washing, coverslips were mounted with anti-fading mounting media (DAKO). Visualization and quantification of apoptotic-positive cells was done under fluorescence microscopy using Axioplan fluorescence microscope (Zeiss). A minimum of 10 high magnification fields (x40) per section, 3-4 thin sections per each heart, and four to five mice per experimental group were examined to determine the percentage of TUNEL-positive nuclei.

Quantitative real-time PCR (qPCR): Total RNA was extracted from myocardial tissue or from isolated cardiac myocytes using the Qiagen miRNeasy Mini Kit (catalogue # 217006). [3, 6] RNA was treated

on column containing DNase to eliminate contaminating genomic DNA. The cDNA was synthesized using High Capacity cDNA Reverse Transcription Kit (Life tech, catalogue # 4368814). Transcript levels were determined by qPCR using specific TaqMan gene expression assays or SYBR Green specific primers, and normalized to glyceraldehyde-3-phosphate dehydrogenase (*Gapdh*) mRNA levels. All reactions were performed in triplicates and in four to six mice per group. The ΔCT method was used to calculate the normalized gene expression value (normalized to *Gapdh*). Data in the experimental groups were presented as fold change relative to the control samples. Taqman probes and SYBR Green primers are detailed in Online Table I.

Immunoblotting: Expression levels of the proteins of interest in mouse heart samples and isolated cardiac myocytes were detected and quantified by immunoblotting, as described. [3, 4, 6] Briefly, tissues were lysed in a RIPA buffer (PIERCE, Rockford, IL, catalogue #89900) containing protease and phosphatase inhibitors (cØmplete and phosSTOP; Roche Molecular Biochemicals, catalogue # 11-873-580-001 and # 04-906-837-001, respectively). The samples were homogenized using a hand-held homogenizer and lysed on a rotator at 4 °C for 20 minutes. The cell debris were pelleted by centrifugation at 12,000 rpm for 15 min at 4 °C. Protein concentration was measured by Bio-Rad DC Protein Assay Kit (Bio-Rad Laboratories, catalogue # 5000111). Protein extracts were heated in a Laemmli buffer at 95 °C for 5 min. Aliquots of 30-50 μg of each protein extract were loaded onto SDS/PAGE gels, separated by electrophoresis, and transferred to nitrocellulose membranes. The membranes were probed with primary antibodies against the proteins of interest and the corresponding HRP conjugated secondary antibodies (the list of the antibodies is provided in Online Table I). Signals were detected by chemiluminescence using the LI-COR Odyssey Fc imaging system (LI-COR Biotechnology). Probes were stripped off the membranes upon incubation in Restore PLUS Western Blot Stripping Buffer (Thermo Scientific, Hudson, New Hampshire, catalogue #46430) at room temperature, and the membranes were reprobed with antibodies against the loading control protein GAPDH or tubulin α1a (TUB1A1). Intensity of the specific bands was quantified using the Image J Studio™ software. Each lane read out was normalized to its corresponding band of the loading control. Data in the experimental groups were presented as the fold change relative to the control samples.

Cell protein sub-fractionation and immunoblotting: Nuclear and cytosolic proteins were extracted using a commercial kit (ProteoExtract®, Calbiochem, catalogue # 539790). [10] All steps were conducted at 4 °C. The hearts were minced and homogenized in a dounce glass homogenizer in 1 mL of a cold Extraction Buffer complemented with protease inhibitors cocktail provided in the kit and with phosphatase inhibitors cocktail, as described above. After incubation and gentle rocking for 20 min, the homogenates were centrifuged at 18,000g for 20 min to pellet the membrane and nuclear fractions and to collect the supernatant containing the cytosolic proteins. After two washes, the pellets were resuspended in 100 µL of an ice-cold buffer containing HEPES (pH7.9), $MgCl_2$, NaCl, EDTA, Glycerol, Sodium OrthoVanadate, plus proteinase inhibitors cocktail. After gentle mixing for 20 min and centrifugation at 18,000g for 20 min, the supernatant containing nuclear proteins was collected.

RNA-Sequencing (RNA-Seq): RNA-sequencing was performed in the whole heart ribosome-depleted RNA extracts from the 2-week old WT and *Lmna*$^{-/-}$ mice on an Illumina platform, as published with minor modifications. [3, 6] In brief, ribosome-depleted RNA was extracted from the whole heart and analyzed for integrity on an Agilent Bioanalyser RNA chip. Samples with a RNA Integrity Number (RIN) read out of more than 8 were used to prepare sequencing library using the Illumina TruSeq stranded total RNA library preparation kit. The samples were sequenced on the Illumina HiSeq 4000 instrument using the paired-end sequencing reagents to generate 100 base pair runs.

Raw RNA sequencing reads were mapped to the Mouse reference genome build 10 (UCSC mm10/GRCm38) by Tophat2. [11] Gene expression was assessed using Cufflinks2 and the GENCODE gene model. [11, 12] Counts were presented as fragments per kilobase of transcript per million mapped fragments (FPKM). Gene expression profiles were normalized using the quantile normalization method as implemented in the R statistical system. Only transcripts that exceeded 1 FPKM in at least one sample were included in the subsequent analyses. Differentially expressed transcripts (DETs) were identified using the edgeR analysis package in R statistical program with the significance level set at $q<0.05$ and the fold change at > 1.25, using the R statistical system. Quality control and data visualization were assessed by principal components analysis (PCA) and hierarchical clustering in R. GENE-E software

(http://www.broadinstitute.org/cancer/software/GENE-E) was used to generate the heatmaps from the raw FPKM values and the Graph Pad Prism was used to generate the volcano plots. Enriched upstream regulators and transcription factor binding sequence motifs were inferred using the following programs: Gene Set Enrichment (GSEA, version 2.2.3, http://software.broadinstitute.org/gsea/); Transcription factor binding motifs TRANSFAC, [13] Molecular Signature Database (MSigDB) using the compute overlap function for transcription factor targets [14-16] and the Ingenuity Pathway Analysis® (IPA, Qiagen). The list of TF target genes dysregulated in the *Lmna*$^{-/-}$ mouse hearts was generated by combining targets identified by GSEA and IPA. Gene Ontology (GO) analyses of FOXO TFs targets genes were conducted using ConsensusPathDB (release MM9-http://cpdb.molgen.mpg.de/MCPDB), [17, 18 19] and GO terms were gathered according to their similarities using REVIGO (http://revigo.irb.hr/). [20] Circos plot was generated in R using the GO-Chord option.

***AAV9-mediated In vivo* suppression of FOXO TFs in the heart:** A short hairpin RNA (shRNA) that has been shown to targets FOXO1 and FOXO3 in independent studies [21, 22] was cloned into AAV9 vectors downstream to a U6 promoter (VectoBiolab). The construct also contained a green fluorescence protein (GFP) expression cassette regulated by a CMV promoter. Control AAV9 vectors contained either a GFP or a scrambled shRNA expression cassette. Sequence of the shRNA against FOXO1 and 3 and scrambled shRNA are presented in Online Table I.

To knock down expression of FOXO1 and FOXO3 in the heart, recombinant AAV9 constructs at a titer of $0.5x10^{11}$ vector genomes per gram of body weight (vg/g) were injected subcutaneously at the nape of the neck into neonatal mice. Three sequential injections at P2, P4, and P6 postnatal days were made, delivering a total of 1.5×10^{11} vg/g to each mouse. Control AAV9 vectors where inject at the same dosage and time points. The early time point was chosen as the *Lmna*$^{-/-}$ have a poor survival rate beyond 4 weeks and almost all die within 8 weeks. [1, 2] Thus, the early injections enabled sufficient time for gene expression through the recombinant AAV9 vectors, prior to the onset of the cardiac phenotype. Serial injections, performed prior to complete immune competency, are expected to enhance transduction efficiency by targeting the newly formed cardiac myocytes in the early neonatal period. [23] The viral titer was chosen

based on the established dose for an efficient transduction of cardiac myocytes while avoiding toxicity. [24-26]

Cytokines measurement: Cytokine and chemokine levels in the heart of 2 weeks old WT and *Lmna*$^{-/-}$ mice were measured using the Milliplex MAP Mouse Cytokine/Chemokine 32-plex assay (Millipore) according to manufacturer's protocol (MCYTMAG-70K-PX32) (Antibody Based Proteomics Core at Baylor College of Medicine, www.bcm.edu/centers/cancer-center/research/shared-resources/antibody-based-proteomics).

Mitochondrial Electron Chain Transport (ETC) Activity: Enzymatic activity of the mitochondrial ETC was assessed in the heart of 2-week old WT and *Lmna*$^{-/-}$ mice, as published. [27] In brief, hearts were homogenized on ice by gentle douncing in a homogenization buffer (120mM KCl, 20mM HEPES, 1mM EGTA, pH7.4), centrifuged at 600g and 4°C for 10 minutes, and the supernatants were used to perform the enzymatic measurements. The specific substrate of each ETC complex was added to the supernatant and the activity was measured by colorimetric assays using a monochromator microplate reader (Tecan M200) at 30 °C in a volume of 175 µL. Complex I activity was determined upon measuring oxidation of NADH at 340 nm using ferricyanide as the electron acceptor in a mixture of 25 mM potassium phosphate (pH 7.5), 0.2 mM NADH, and 1.7 mM potassium ferricyanide (NADH:ubiquinone oxidoreductase). Complex II activity (succinate dehydrogenase) was assessed by determining by the rate of reduction of the artificial electron acceptor 2,6-dichlorophenol-indophenol (DCIP) at 600 nm in a mixture of 25 mM potassium phosphate (pH 7.5), 20 mM succinate, 0.5 mM DCIP, 10 µM rotenone, 2 µg/mL antimycin A, and 2 mM potassium cyanide. Complex III activity (Ubiquinol/cytochrome *C* oxidoreductase) was determined by assessing reduction of cytochrome *C* (C*C*) at 550 nm in a mixture of 25 mM potassium phosphate (pH 7.5), 35 µM reduced decylubiquinone, 15 µM C*C*, 10 µM rotenone, and 2 mM potassium cyanide. Cytochrome C oxidase activity at 550 nm was measured in a mixture of 10 mM potassium phosphate (pH 7.5) and 0.1 mM reduced C*C* to determine Complex IV activity. Finally, reduction of 5,5'-dithiobis (2-nitrobenzoic acid) (DTNB) at 412 nm, which is coupled to the reduction of acetyl-CoA by citrate synthase in the presence of oxaloacetate in a mixture of 10 mM potassium phosphate (pH 7.5), 100

mM DTNB, 50 mM acetyl-CoA, and 250 mM oxaloacetate, was used to determine the Citrate Synthase activity. All activities were calculated as nmoles/min/mg protein, normalized to citrate synthase activity, and expressed as a percentage of WT activity. Experiments were performed on four independent samples for each genotype.

ETC complexes assembly immunoblotting: ETC complexes assembly was assessed by immunoblotting of specific subunit of each of the five ETC complexes using the Total OXPHOS Rodent WB Antibody Cocktail (Abcam, #ab110413). These specific subunits are labil, and therefore, are decreased or not detected when complexes are not assembled. Frozen heart tissue were solubilized in SDS buffer (2% SDS, 10% glycerol, 50 mM Tris pH 6.8, protease inhibitor cØmplete) and centrifuged at 4°C and 13,000 rpm for 5 minutes. Supernatant were collected and protein present were quantified. Aliquotes of 50 mM dithiothreitol were added to 20 µg of proteins before loading onto a 4-15% acrylamide gel for SDS-page electrophoresis. Proteins were then transferred on PVDF membrane by CAPS electroblotting in a buffer containing 10 mM 3-[cyclohexylamino]-1-propane sulfonic acid (Sigma C2632) pH 11 and 10 % Methanol. The membrane was then blocked overnight with PBS-5% milk, probed with 6.0 µg/mL of antibodies cocktail for 24 hours at 4°C before incubation with secondary antibody anti-mouse HRP-conjugated. Chemiluminescence signal was acquired using the LI-COR Odyssey Fc imaging system. Analysis was performed using Image Studio software. Loading control was assessed by staining the membrane with Red Ponceau. Proteins were extracted from 2 animal hearts per experimental group and Rat mitochondrial extract was used as positive control.

ATP measurement: To assess if ATP production was impaired in the *Lmna*$^{-/-}$ mouse heart, ATP was measured using the ATP Assay Kit (Abcam, #ab83355) according to manufacturer's instruction. Briefly, 20mg of frozen heart tissue were homogenized on ice using a hand-held homogeneizer in ice-cold 2M Perchloric acid (PCA). Homogenate were then incubated on ice for 45 min before centrifugation at 13,000 g for 2 min at 4°C. Supernatant were collected and PCA neutralized with of ice-cold 2M KOH. pH of the samples was measured and adjusted as necessary to range between 6.5 and 8. Samples were then

centrifugated again at 13,000 g for 2 min at 4°C and used for the colorimetric assay. 5 samples of heart tissue were used per experimental group.

Statistical analyses: Data that followed a Gaussian distribution pattern were presented as mean ± SEM and were compared by t-test and one-way ANOVA. Otherwise, data were presented as the median values and compared by Kruskall-Wallis test, as were the categorical data. Survival rates were analyzed by constructing Kaplan-Meier survival plots and comparing the survival rate by Log-rank (Mantel-Cox) test.

REFERENCES

1. Sullivan T, Escalante-Alcalde D, Bhatt H, Anver M, Bhat N, Nagashima K, Stewart CL, Burke B. Loss of a-type lamin expression compromises nuclear envelope integrity leading to muscular dystrophy. *The Journal of cell biology*. 1999;147:913-920
2. Nikolova V, Leimena C, McMahon AC, Tan JC, Chandar S, Jogia D, Kesteven SH, Michalicek J, Otway R, Verheyen F, Rainer S, Stewart CL, Martin D, Feneley MP, Fatkin D. Defects in nuclear structure and function promote dilated cardiomyopathy in lamin a/c-deficient mice. *The Journal of clinical investigation*. 2004;113:357-369
3. Gurha P, Chen X, Lombardi R, Willerson JT, Marian AJ. Knockdown of plakophilin 2 downregulates mir-184 through cpg hypermethylation and suppression of the e2f1 pathway and leads to enhanced adipogenesis in vitro. *Circulation research*. 2016;119:731-750
4. Lombardi R, Chen SN, Ruggiero A, Gurha P, Czernuszewicz GZ, Willerson JT, Marian AJ. Cardiac fibro-adipocyte progenitors express desmosome proteins and preferentially differentiate to adipocytes upon deletion of the desmoplakin gene. *Circulation research*. 2016;119:41-54
5. Ruggiero A, Chen SN, Lombardi R, Rodriguez G, Marian AJ. Pathogenesis of hypertrophic cardiomyopathy caused by myozenin 2 mutations is independent of calcineurin activity. *Cardiovascular research*. 2013;97:44-54
6. Chen SN, Gurha P, Lombardi R, Ruggiero A, Willerson JT, Marian AJ. The hippo pathway is activated and is a causal mechanism for adipogenesis in arrhythmogenic cardiomyopathy. *Circulation research*. 2014;114:454-468
7. Tsybouleva N, Zhang L, Chen S, Patel R, Lutucuta S, Nemoto S, DeFreitas G, Entman M, Carabello BA, Roberts R, Marian AJ. Aldosterone, through novel signaling proteins, is a fundamental molecular bridge between the genetic defect and the cardiac phenotype of hypertrophic cardiomyopathy. *Circulation*. 2004;109:1284-1291
8. Karmouch J, Zhou QQ, Miyake CY, Lombardi R, Kretzschmar K, Bannier-Helaouet M, Clevers H, Wehrens XHT, Willerson JT, Marian AJ. Distinct cellular basis for early cardiac arrhythmias, the cardinal manifestation of arrhythmogenic cardiomyopathy, and the skin phenotype of cardiocutaneous syndromes. *Circulation research*. 2017;121:1346-1359

9. Garcia-Gras E, Lombardi R, Giocondo MJ, Willerson JT, Schneider MD, Khoury DS, Marian AJ. Suppression of canonical wnt/beta-catenin signaling by nuclear plakoglobin recapitulates phenotype of arrhythmogenic right ventricular cardiomyopathy. *The Journal of clinical investigation*. 2006;116:2012-2021
10. Lombardi R, Bell A, Senthil V, Sidhu J, Noseda M, Roberts R, Marian AJ. Differential interactions of thin filament proteins in two cardiac troponin t mouse models of hypertrophic and dilated cardiomyopathies. *Cardiovascular research*. 2008;79:109-117
11. Kim D, Pertea G, Trapnell C, Pimentel H, Kelley R, Salzberg SL. Tophat2: Accurate alignment of transcriptomes in the presence of insertions, deletions and gene fusions. *Genome Biol*. 2013;14:R36
12. Trapnell C, Williams BA, Pertea G, Mortazavi A, Kwan G, van Baren MJ, Salzberg SL, Wold BJ, Pachter L. Transcript assembly and quantification by rna-seq reveals unannotated transcripts and isoform switching during cell differentiation. *Nat Biotechnol*. 2010;28:511-515
13. Xie X, Lu J, Kulbokas EJ, Golub TR, Mootha V, Lindblad-Toh K, Lander ES, Kellis M. Systematic discovery of regulatory motifs in human promoters and 3' utrs by comparison of several mammals. *Nature*. 2005;434:338-345
14. Subramanian A, Tamayo P, Mootha VK, Mukherjee S, Ebert BL, Gillette MA, Paulovich A, Pomeroy SL, Golub TR, Lander ES, Mesirov JP. Gene set enrichment analysis: A knowledge-based approach for interpreting genome-wide expression profiles. *Proceedings of the National Academy of Sciences of the United States of America*. 2005;102:15545-15550
15. Liberzon A, Subramanian A, Pinchback R, Thorvaldsdottir H, Tamayo P, Mesirov JP. Molecular signatures database (msigdb) 3.0. *Bioinformatics*. 2011;27:1739-1740
16. Liberzon A, Birger C, Thorvaldsdottir H, Ghandi M, Mesirov JP, Tamayo P. The molecular signatures database (msigdb) hallmark gene set collection. *Cell Syst*. 2015;1:417-425
17. Kamburov A, Pentchev K, Galicka H, Wierling C, Lehrach H, Herwig R. Consensuspathdb: Toward a more complete picture of cell biology. *Nucleic Acids Res*. 2011;39:D712-717
18. Kamburov A, Stelzl U, Lehrach H, Herwig R. The consensuspathdb interaction database: 2013 update. *Nucleic Acids Res*. 2013;41:D793-800
19. Herwig R, Hardt C, Lienhard M, Kamburov A. Analyzing and interpreting genome data at the network level with consensuspathdb. *Nat Protoc*. 2016;11:1889-1907
20. Supek F, Bosnjak M, Skunca N, Smuc T. Revigo summarizes and visualizes long lists of gene ontology terms. *PloS one*. 2011;6:e21800
21. Hribal ML, Nakae J, Kitamura T, Shutter JR, Accili D. Regulation of insulin-like growth factor-dependent myoblast differentiation by foxo forkhead transcription factors. *The Journal of cell biology*. 2003;162:535-541
22. Renault VM, Thekkat PU, Hoang KL, White JL, Brady CA, Kenzelmann Broz D, Venturelli OS, Johnson TM, Oskoui PR, Xuan Z, Santo EE, Zhang MQ, Vogel H, Attardi LD, Brunet A. The pro-longevity gene foxo3 is a direct target of the p53 tumor suppressor. *Oncogene*. 2011;30:3207-3221
23. Alkass K, Panula J, Westman M, Wu TD, Guerquin-Kern JL, Bergmann O. No evidence for cardiomyocyte number expansion in preadolescent mice. *Cell*. 2015;163:1026-1036

24. Schobesberger S, Wright P, Tokar S, Bhargava A, Mansfield C, Glukhov AV, Poulet C, Buzuk A, Monszpart A, Sikkel M, Harding SE, Nikolaev VO, Lyon AR, Gorelik J. T-tubule remodelling disturbs localized beta2-adrenergic signalling in rat ventricular myocytes during the progression of heart failure. *Cardiovascular research*. 2017;113:770-782
25. Guo Y, VanDusen NJ, Zhang L, Gu W, Sethi I, Guatimosim S, Ma Q, Jardin BD, Ai Y, Zhang D, Chen B, Guo A, Yuan GC, Song LS, Pu WT. Analysis of cardiac myocyte maturation using casaav, a platform for rapid dissection of cardiac myocyte gene function in vivo. *Circulation research*. 2017
26. Reynolds JO, Quick AP, Wang Q, Beavers DL, Philippen LE, Showell J, Barreto-Torres G, Thuerauf DJ, Doroudgar S, Glembotski CC, Wehrens XH. Junctophilin-2 gene therapy rescues heart failure by normalizing ryr2-mediated ca2+ release. *International journal of cardiology*. 2016;225:371-380
27. Donti TR, Stromberger C, Ge M, Eldin KW, Craigen WJ, Graham BH. Screen for abnormal mitochondrial phenotypes in mouse embryonic stem cells identifies a model for succinyl-coa ligase deficiency and mtdna depletion. *Disease models & mechanisms*. 2014;7:271-280

Online Table I

A. List of primers

Gene Identity	Ref/Oligonucleotidic Sequence
Taqman probes:	
Gapdh	Mm99999915-g1
Tgfb1	Mm01178820-m1
Ctgf	Mm01192932-g1
Col3a1	Mm01254476-m1
Col1a1	Mm00801666-g1
SYBR Green primers:	
***Lmna*-WT**	fwd: 5'- TGGCGGTAGAGGAAGTCGATGAAG-3' rev 5'AGGAAGGAGGACAGGGAGTTCAAC-3'
***Lmna*-KO**	fwd 5'-GGCGGTAGAGGAAGTCGATGAAG-3' rev 5'-TGACCCATGGCGATGCCTGCTTG-3'
Fkbp5	fwd 5'- TCCACTACAAAGGGATGTTGTCA-3' rev 5'-CGAGCCATAAGCATATTCTGGTT-3'
Myl4	fwd 5'-AAGAAACCCGAGCCTAAGAAGG-3' rev 5'-TGGGTCAAAGGCAGAGTCCT-3'
Prg4	fwd 5'- CAGGTTTCATCTCAAGATTT-3' rev 5'- TGTAGTGCAGACTCTCTTGA-3'
Atf3	fwd 5'-CCCCTGGAGATGTCAGTCAC-3' rev 5'- CGGTGCAGGTTGAGCATGT-3'
Hmox1	fwd 5'-CATGAAGAACTTTCAGAAGGG-3' rev 5'-TAGATATCTGACCCAGTTC-3'
Myh7	fwd 5'- ACTGTCAACACTAAGAGGGTCA-3' rev 5'- TTGGATGATTTGATCTTCCAGGG-3'
Psat1	fwd 5'-AAGCCACCAAGCAAGTGGTTA-3' rev 5'-GATGCCGAGTCCTCTGTAGTC-3'
Abi3bp	fwd 5'- TTGAAAGTGCACATCAATAC-3' rev 5'- ACTACAGCCTCTGTGAATTT-3'
Btg2	fwd 5'- ATGAGCCACGGGAAGAGAAC-3' rev 5'- AGCGCCCTACTGAAAACCTTG-3'
Myc	fwd 5'- CTGCTCTCCATCCTATGTT-3' rev 5'- AGTAACTCGGTCATCATCTC-3'
Cryba4	fwd 5'- GGGTGGCAACACAGCCTAC-3' rev 5'- TTGAGTCGCGGTGGTTAGC-3'
Lrtm1	fwd 5'-AAGGACAACCCTTGGATTTGTG-3' rev 5'-ACAGTTCGTGAGGAATGGAGAG-3'
Itgb6	fwd 5'-CAGGTCCGCCAAACTGAAGAT-3' rev 5'-TGTTGAGGTCGTCATCCATAGA-3'

Aurka	fwd 5'-GAGAGTTGAAGATTGCAGAC-3' rev 5'-TAGGAACTCATAGCAGAGAAC-3'
Lmna	fwd 5'- TCCCACCGAAGTTCACCCTA-3' rev 5'- TGGAGTTGATGATGAGAGCGGTG-3'
Cxcl1	fwd 5'- CTGGGATTCACCTCAAGAACATC-3' rev 5'- CAGGGTCAAGGCAAGCCTC-3'
Cxcl2	fwd 5'- ACAGAAGTCATAGCCACTCT-3' rev 5'- ACATCAGGTACGATCCAG-3'
Ccl2	fwd 5'- AAGCTGTAGTTTTTGTCACC-3' rev 5'- TGCATTAGCTTCAGATTTAC-3'
Il6	fwd 5'- GTCTTCTGGAGTACCATAGC-3' rev 5'- GCTTATCTGTTAGGAGAGCA-3'
Lif	fwd 5'- ATTGTGCCCTTACTGCTGCTG-3' rev 5'- GCCAGTTGATTCTTGATCTGGT-3'
Ndufaf1	fwd 5'- TTTGTGGGTAGTCACTGTGTAGA-3' rev 5'- TGTCCTTGTAAGCCCTCTTCAG-3'
Ccnb1	fwd 5'- AAGGTGCCTGTGTGTGAACC-3' rev 5'-GTCAGCCCCATCATCTGCG-3'
Ccnb2	fwd 5'-CCAAGTCCATTCCAAGTTTC-3' rev 5'-CATCTCCTCATATTTGGAAGC-3'
Cdkn1a	fwd 5'- CCTGGTGATGTCCGACCTG-3' rev 5'- CCATGAGCGCATCGCAATC-3'
Foxo1	fwd 5'- CCCAGGCCGGAGTTTAACC-3' rev 5'- GTTGCTCATAAAGTCGGTGCT-3'
Foxo3	fwd 5'- CTGGGGGAACCTGTCCTATG -3' rev 5'-TCATTCTGAACGCGCATGAAG -3'
Foxo4	fwd 5'- CTTCCTCGACCAGACCTCG-3' rev 5'-ACAGGATCGGTTCGGAGTGT-3'
Slc24a2	fwd 5'- GACAAGATTCGAGATTACACCCC-3' rev 5'-TGCAGAATGATGGCACCTTTC-3'
Nr4a2	5'- GTGTTCAGGCGCAGTATGG-3' rev 5'-TGGCAGTAATTTCAGTGTTGGT-3'
Rasgef1b	fwd 5'-TCTGGAAGCCCTTATCCAACA -3' rev 5'-GTGGCAAACCTTAGCCATGAG-3'
Gadd45b	fwd 5'-CAACGCGGTTCAGAAGATGC-3' rev 5'-GGTCCACATTCATCAGTTTGGC-3'
Sqstm1	fwd 5'-ATGTGGAACATGGAGGGAAGA-3' rev 5'-GGAGTTCACCTGTAGATGGGT-3'
Per1	fwd 5'-TGAAGCAAGACCGGGAGAG -3' rev 5'-CACACACGCCGTCACATCA -3'
Etv5	fwd 5'-TCAGTCTGATAACTTGGTGCTTC-3' rev 5'-GGCTTCCTATCGTAGGCACAA-3'
Nfkbia	fwd 5'-TGAAGGACGAGGAGTACGAGC-3' rev 5'-TTCGTGGATGATTGCCAAGTG-3'
Nr4a1	fwd 5'-CTCCCCGAGCCAGACTTATGA-3' rev 5'-TGTCACGGTTCGGAGAGGT-3'
Junb	fwd 5'-CTATCGGGGTCTCAAGGGTC-3' rev 5'-CTGTTGGGGACGATCAAGC-3'
Mt2	fwd 5'-GCCTGCAAATGCAAACAATGC -3' rev 5'-AGCTGCACTTGTCGGAAGC-3'

Maff	fwd 5'-TGGATCCCTTATCTAGCA -3' rev 5'-CTCGGACTTCTGCTTCT-3'
Gabarapl1	fwd 5'-GGACCACCCCTTCGAGTATC-3' rev 5'-CCTCTTATCCAGATCAGGGACC-3'
Cited2	fwd 5'-CGCCAGGTTTAACAACTCCCA-3' rev 5'-TGCTGGTTTGTCCCGTTCAT-3'
Bcl2l11	fwd 5'-CCCGGAGATACGGATTGCAC-3' rev 5'-GCCTCGCGGTAATCATTTGC-3'
Bbc3	fwd 5'-ACGACCTCAACGCGCAGTACG-3' rev 5'-GTAAGGGGAGGAGTCCCATGAAG-3'
Bcl6	fwd 5'-CCGGCACGCTAGTGATGTT-3' rev 5'-TGTCTTATGGGCTCTAAACTGCT-3'
Tnfsf10	fwd 5'- ATGGTGATTTGCATAGTGCTCC-3' rev 5'-GCAAGCAGGGTCTGTTCAAGA-3'
Ndufaf1	fwd 5'- TTTGTGGGTAGTCACTGTGTAGA -3' rev 5'- TGTCCTTGTAAGCCCTCTTCAG -3'
Ndufaf4	fwd 5'- CACCGGAGTCAGTATCCAGAA -3' rev 5'- GGTTCAACTTTTACCGGCAAGG -3'
Ndufs4	fwd 5'- CTGCCGTTTCCGTCTGTAGAG -3' rev 5'- TGTTATTGCGAGCAGGAACAAA -3'
Ndufaf3	fwd 5'- ATGGCTACTGCTCTAGGATTTCG -3' rev 5'- CCGCTGGTATAACTCATCGTC -3'
Ndufs8	fwd 5'- AGTGGCGGCAACGTACAAG -3' rev 5'- TCGAAAGAGGTAACTTAGGGTCA -3'
Ndufb2	fwd 5'- CCCCGGTACAGGGAGTTTC -3' rev 5'- GCCAAAATCGCCAAAGAATCCA -3'
Ndufb10	fwd 5'- GATTCTTGGGACAAGGATGTGT -3' rev 5'- CCTTCGTCAAGTAGGTGATGGG -3'
Ndufs1	fwd 5'- AGGATATGTTCGCACAACTGG -3' rev 5'- TCATGGTAACAGAATCGAGGGA -3'
Ndufa2	fwd 5'- TTGCGTGAGATTCGCGTTCA -3' rev 5'- ATTCGCGGATCAGAATGGGC -3'
Ndufa3	fwd 5'- ATGGCCGGGAGAATCTCTG -3' rev 5'- AGGGGCTAATCATGGGCATAAT -3'
Gapdh	fwd 5'- TGGCAAAGTGGAGATTGTTGC-3' rev 5'-AAGATGGTGATGGGCTTCCCG-3'

B. List of Antibodies

Antibodies	**Supplier**	**Reference**
LMNA	Abcam	# 26300
Emerin (FL-254)	Santa Cruz Biotechnology	# sc-15378
TUB1A1 (11H10)	Cell Signaling Technology	# 21252
GAPDH	Abcam	# 82245
FOXO3 (D19D7)	Cell Signaling Technology	# 12829

FOXO3 (75D8)	Cell Signaling Technology	#2497
FOXO1 (C29H4)	Cell Signaling Technology	# 2880
phosphoFOXO (4G6)	Cell Signaling Technology	# 2599
FOXO4	ProteinTech	21535-1-AP
ACTN2	Sigma	A7811
JPH2	Invitrogen	#40-5300

Anti-Rabbit IgG, Alexa Fluor 594	Life technology	21207
Anti-Mouse IgG, Alexa Fluor 488	Life technology	21202
Anti-rabbit IgG HRP linked antibody	Cell Signaling Technology	# 7074
Anti-mouse IgG HRP linked antibody	Cell Signaling Technology	# 7076

C. ShRNA sequence

FOXO1 and 3 shRNA sequence: 5’- GGATAAGGGCGACAGCAAC-3’

Scrambled-shRNA sequence: 5'-CAACAAGATGAAGAGCACCAA-3'

Online Table II

Echocardiographic variables in 2-week old control wild type and *Lmna*$^{-/-}$ Mice

	WT	*Lmna* $^{-/-}$	*p*
N	15	14	N/A
M/F	9/6	9/5	1.000
Age (days)	13.5 ± 1.3	13.7 ± 1.3	0.708
Body weight (g)	7.08 ± 1.6	5.9 ± 1.3	0.037
HR (bpm)	506 ± 63	512 ± 76	0.839
IVST(mm)	0.55 ± 0.08	0.52 ± 0.08	0.356
PWT (mm)	0.57 ± 0.09	0.53 ± 0.08	0.209
LVEDD (mm)	2.48 ± 0.31	2.37 ± 0.33	0.377
LVEDDi (mm/g)	0.36 ± 0.06	0.41 ± 0.06	0.032
LVESD (mm)	1.22 ± 0.19	1.22 ± 0.26	0.979
LVESDi (mm/g)	0.18 ± 0.03	0.21 ± 0.04	0.059
FS (%)	51.03 ± 2.92	49.17 ± 5.12	0.248
LVM (mg)	32.66 ± 11.95	27.81 ± 9.67	0.248
LVMi (mg/g)	4.71 ± 1.46	4.76 ± 1.52	0.938

Abbreviations: HR: heart rate; bpm: beats per minutes; IVST: interventricular septal thickness; PWT: posterior wall thickness; LVEDD: left ventricular end diastolic diameter; LVEDDi: LVEDD divided by the body weight; LVESD: left ventricular end systolic diameter; LVESDi: LVESD divided for the body weight; FS: fractional shortening; LVM: left ventricular mass; LVMi: LVM divided by the body weight.

Online Table III

Enrichment of conserved cis-regulatory motifs in Differentially Expressed Transcripts

Enrichment of conserved *cis* -regulatory motifs in up-regulated DETs

TFs name	Gene Set Name	Binding motif	Description	# Genes in Overlap (k)	FDR
FOXO4	V$FOXO4_01	TTGTTT	Promoter regions containing the motif TTGTTT which matches annotation for MLLT7: myeloid/lymphoid or mixed-lineage leukemia (trithorax homolog, Drosophila); translocated to, 7	99	1.19E-33
NFAT	V$NFAT_Q4_01	TGGAAA	Promoter regions containing the motif TGGAAA which matches annotation for NFAT:NFATC	80	3.92E-23
AP1	V$AP1_C	TGANTCA	Promoter regions containing the motif TGANTCA which matches annotation for JUN: jun oncogene	60	4.41E-22
E12	V$E12_Q6	CAGGTG	Promoter regions containing the motif CAGGTG which matches annotation for TCF3: transcription factor 3 (E2A immunoglobulin enhancer binding factors E12/E47)	88	8.43E-21
Unknown	UNKNOWN	AACTTT	Promoter regions containing motif AACTTT. Motif does not match any known transcription factor	74	1.03E-19
FREAC2	V$FREAC2_01	RTAAACA	Promoter regions containing the motif RTAAACA which matches annotation for FOXF2: forkhead box F2	51	1.64E-19
AP4	V$AP4_Q5	CAGCTG	Promoter regions containing the motif CAGCTG which matches annotation for REPIN1: replication initiator 1	61	1.45E-16
MAZ	V$MAZ_Q6	GGGAGGRR	Promoter regions containing the motif GGGAGGRR which matches annotation for MAZ: MYC-associated zinc finger protein (purine-binding transcription factor)	74	1.91E-15
PAX4	V$PAX4_03	GGGTGGRR	Promoter regions containing the motif GGGTGGRR which matches annotation for PAX4: paired box gene 4	54	2.01E-15
TATA	V$TATA_01	TATAAA	Promoter regions containing the motif TATAAA which matches annotation for TAF:TATA	54	2.01E-15

Enrichment of conserved *cis* -regulatory motifs indown-regulated DETs

TFs name	Gene Set Name	Binding motif	Description	# Genes in Overlap (k)	FDR
E2F	V$E2F_Q6	TTTSGCGS	Promoter regions containing motif TTTSGCGS. Motif does not match any known transcription factor	9	4.08E-04
E2F	V$E2F_Q4	TTTSGCGS	Promoter regions containing motif TTTSGCGS. Motif does not match any known transcription factor	9	4.08E-04
Unknown	UNKNOWN	TTTNNANAGCYR	Promoter regions containing motif TTTNNANAGCYR. Motif does not match any known transcription factor	7	5.36E-04
NF1	V$NF1_Q6	TGCCAAR	Promoter regions containing the motif TGCCAAR which matches annotation for NF1: neurofibromin 1 (neurofibromatosis, von Recklinghausen disease, Watson	14	7.74E-04
E2F1-DP1-RB	V$E2F1_Q4_01	TTTSGCGSG	Promoter regions containing the motif TTTSGCGSG which matches annotation for E2F;TFDP1: transcription factor Dp-1	8	7.74E-04
E2F1-DP1-RB	V$E2F1DP1RB_01	TTTSGCGC	Promoter regions containing the motif TTTSGCGC which matches annotation for E2F1: E2F transcription factor 1; TFDP1: transcription factor Dp-1;RB1: retinoblastoma 1 (including osteosarcoma)	8	7.74E-04
E2F1-DP1-RB	V$E2F1DP2_01	SGCGSSAAA	Promoter regions containing the motif SGCGSSAAA which matches annotation for E2F1: E2F transcription factor 1;TFDP1: transcription factor Dp-1;RB1: retinoblastoma 1 (including osteosarcoma)	7	7.74E-04
Unknown	UNKNOWN	KRCTCNNNNMANAGC	Promoter regions containing motif KRCTCNNNNMANAGC. Motif does not match any known transcription factor	5	7.74E-04
E2F	V$E2F_Q3_01	TTTSGCGSG	Promoter regions containing the motif TTTSGCGSG which matches annotation for E2F:TFDP1: transcription factor Dp-1	8	7.74E-04
E2F	V$E2F_Q4_01	NCSCGCSAAAN	Promoter regions containing the motif NCSCGCSAAAN which matches annotation for E2F:TFDP1: transcription factor Dp-1	8	7.74E-04

Up and down-regulated DETs were analysed for enrichment of conserved upstream cis-regulatory motifs by using the MSigDB from GSEA. The conserved transcription factor binding sites and conserved motifs analysis was restricted to the promoter region around transcription start site (4kb window, -2 kb; +2kb).

Top ten of the significantly over-represented *cis*-regulatory motifs are presented in the tables. Over-representation is calculated by hypergeometric distribution of overlapping genes (k) over all genes in the gene universe, after correction for multiple hypothesis testing.

Online Table IV

Upstream regulators of DETs in *Lmna*$^{-/-}$ mice predicted by IPA.

Predicted Activation State	IPA ranking	Upstream Regulator	Activation z-score	p-value of overlap	Target molecules in dataset
Activated	1	CTNNB1	4.577	6.48E-12	APOD,BCL2,BCL2L1,C2orf40,CA3,CD44,CDKN1A,CTGF,CYP1B1,CYR61,DPEP1,EYA2,F2R,FAS,FOXC1,FOXC2,FSTL3,FZD7,GADD45B,GDNF,GLUL,ID4,KLF5,LGALS3,MME,MMP3,MYC,MYCN,MYL4,NR4A1,NR5A2,PCCA,PRDM1,PRSS35,SERPINA3,SERPINE1,SGK1,SLC1A5,SMAD6,SOX17,SPP1,SQSTM1,SYNM,TGFA,TIMP3,TNFRSF19,VCAM1,WIF1,WNT11
	2	CREB1	4.03	2.73E-14	ATF3,AURKA,BCL2,BCL2L1,BTG2,CCNB1,CCNB2,CEBPD,CSRNP1,CYR61,EGR1,ENTPD1,ERRFI1,FOS,FOSB,GADD45B,IRS2,JUNB,KLF5,MIDN,MKI67,MYC,NR4A1,NR4A2,NR4A3,PER1,PPP1R15A,Retnla,Sik1
	3	CREM	3.762	1.18E-09	ATF3,BTG2,CSRNP1,EGR1,ERRFI1,FOS,GADD45B,HAND2,IRS2,JUNB,KLF5,MIDN,NR4A1,NR4A2,PER1,PPP1R15A,RYR2,Sik1,STAR,THBS1
	4	FOXO3	3.755	3.26E-07	Acot1,BNIP3,CDKN1A,CTGF,EGR1,FOS,FOSB,GADD45B,GSTM5,JUNB,LCN2,Mt1,Mt2,NFKBIA,SGK1,
	5	TP53	3.507	3.27E-20	ABCG2,ACER2,ADAM8,ATF3,AURKA,BCL2,BCL2L1,BMX,BNIP3,BTG2,CAMK2N1,Ccl2,CCNB1,CDC7,CDKN1A,CEP55,CITED2,CKAP2,CLU,COL2A1,CTGF,DDIT4,DKK3,DPEP1,DUSP5,EGR1,ENPP2,EPHX1,F2R,FAS,FHL1,FKBP4,FKBP5,FOS,FSTL3,GDF15,GLUL,GNA13,GNL3,GPX3,GSTM5,Hist1h1b,HK2,HMOX1,HRASLS,HSPA1A/HSPA1B,HSPB1,HSPD1,IFI16,IGF1R,IGF2,IGFBP3,IL16,JUNB,KDR,KRT18,KRT8,LGALS3,LOC102724788/PRODH,LOX,MCM2,MIR17HG,MKI67,MMP3,MPZL2,Mt2,MYC,MYL4,NFKBIA,PCCA,PEG10,PERP,PFKFB3,PHLDA1,PHLDA3,PIM1,POLD2,PRC1,PRDM1,PTGDS,PTGS1,PTPRU,RAD51,RBM3,SELP,SERPINA3,SERPINE1,SERPINH1,SGK1,SHROOM3,SLC2A12,SLC6A6,SMAD6,SPHK1,SPP1,TGFA,TGFB2,THBS1,TIMP3,TMEM151A,TMEM43,TNFAIP8,TOP2A,TP53INP1,TPX2,TTK,UHRF1,UNG
	6	EGR1	3.373	8.5E-10	ATF3,CACNA1H,Ccl2,CD44,CDKN1A,CHGB,CXCL3,EREG,FAS,FTL,GDF15,HMOX1,HPSE,IGF2,JUNB,JUND,MYC,SERPINE1,THBS1,VCAM1
	7	ATF4	3.215	8.22E-09	ANGPTL3,ANKRD1,ATF3,CDKN1A,CHAC1,DDIT4,EIF4EBP1,GDF15,LGALS3,MGST1,OSMR,PCK1,PSAT1,PTX3,SLC1A5,SLC38A2,SLC38A3,SLC3A2,SLC7A5,WNT11
	8	RELA	3.102	4.29E-08	ABCG2,ANKRD1,BCL2,BCL2L1,BTG2,CBS/CBSL,Ccl2,CD14,CD44,CDKN1A,CITED2,CXCL3,CXCR4,CYP2B6,FAS,FOS,HMOX1,MYC,NFKBIA,NR4A1,PRDM1,PRKCD,PTGDS,PTX3,SDC4,SLC2A5,VCAM1
	9	SMAD3	3.064	0.0000106	ANKRD1,BCL2,Ccl2,CDKN1A,COL2A1,CTGF,CXCL3,EREG,FOS,FSTL3,JUNB,JUND,MYC,SERPINE1,SPHK1,TGFA,TIMP3
	10	ID2	2.813	0.000929	BCL2,BCL2L1,CCNB1,CD19,CD44,CDKN1A,CXCR4,CXCR6,GADD45B,KLF6,MYC,NR4A1,NR4A3,RAP1GAP
	...				
	29	FOXO4	2.215	0.00513	BNIP3,CDKN1A,CTGF,GADD45B,SGK1
	...				
	96	FOXO1	0.616	2.72E-08	ASPM,BCL2,CCNB1,CCNB2,CDKN1A,CTGF,DEPDC1,DLGAP5,EGR1,FOS,FOSB,GADD45B,GCK,IGF1R,IRS2,ITGA3,ITGB6,JUNB,MMP3,MRPL45,MYC,NDUFAF1,PCK1,PRC1,PRDM1,SGK1,THBS1,UCP1,VCAM1
Inhibited	9	MKL2	-2	0.00000312	BCL2L1,CLDN15,CXCR4,DMKN,EYA2,F2R,GSTM5,Ifitm1,LCN2,MAFK,P2RY1,SELP,SERINC3
	8	HLX	-2.121	6.86E-07	ANKRD1,CCNB1,CYP1B1,EGR1,GDF15,MYC,PAPPA,PRDM1
	7	BACH1	-2.15	0.000246	CXCR4,GCLM,HMOX1,SPP1,SQSTM1
	6	HEY2	-2.193	0.000324	ANKRD1,MYL4,MYL7,NPPA,SLN
	5	SNAI2	-2.219	0.0034	ANKRD1,COL2A1,CTGF,CYR61,ITGA3
	4	GMNN	-2.646	0.00524	CDKN1A,CITED1,DUSP5,FOXF1,IRX3,SOX17,TGFB2,TNFRSF19
	3	SOX1	-2.646	0.00947	CITED1,DUSP5,FOXF1,IRX3,SOX17,TGFB2,TNFRSF19
	2	HOXA10	-3	0.00592	ADM,CA3,ENPP2,IGFBP3,INMT,LCN2,MYCN,NR4A1,XDH
	1	SOX2	-3.443	0.00000136	ATF3,CITED1,CITED2,CTGF,CXCR4,DUSP5,ESRRB,ETV5,FOXF1,GADD45B,GATA6,GCK,GRHL3,H19,IRX3,KDR,KLF6,KRT18,MYCN,NR5A2,PRDM1,PRKCD,SOX17,TGFB2,TIMP3,TNFRSF19

Differentially Expressed Transcripts were analysed using Ingenuity Pathway Analysis (IPA) Software to predict upstream transcriptional regulators under the most stringent setting. Significant upstream regulators are identified based on the literature and curated IPA database. A Fisher's Exact Test p-value calculation of the overlap between the DETs and known targets render the significant overrepresented upstream regulator. Prediction of regulators activation state is inferred based on the direction of the change of knowns target, consistent with the literature and is computed by z-score. In the table are displayed the top 10 predicted activated (in red) and the top ten inhibited (in blue) upstream regulators. IPA ranking (1 to 10) identified from the most to the less significant upstream regulator.

Online Table V

Gene Ontology analysis on FOXO targets genes

Gene Ontology Term		Category, Level	Set Size	Candidates contained	*p* -value	*q* -value
GO:0012501	Programmed Cell Death	BP 4	1320	38 (2.9%)	1.25E-13	5.62E-11
GO:0048523	Negative Regulation of Cellular Process	BP 4	2601	51 (2.0%)	8.62E-12	1.94E-09
GO:0071310	Cellular Response to Organic Substance	BP 4	1019	30 (3.0%)	5.02E-11	7.53E-09
GO:0010941	Regulation of Cell Death	BP 4	986	29 (3.0%)	1.17E-10	1.32E-08
GO:0048522	Positive Regulation of Cellular Process	BP 4	2753	49 (1.8%)	8.91E-10	8.02E-08
GO:0042127	Regulation of Cell Proliferation	BP 4	1021	28 (2.8%)	1.29E-09	9.66E-08
GO:0071241	Cellular Response to Inorganic Substance	BP 4	73	9 (12.3%)	3.30E-09	2.12E-07
GO:0010646	Regulation of Cell Communication	BP 4	1971	38 (1.9%)	1.65E-08	9.28E-07
GO:0009893	Positive Regulation of Metabolic Process	BP 4	1817	36 (2.0%)	2.43E-08	1.22E-06
GO:0007517	Muscle Organ Development	BP 4	352	15 (4.3%)	5.19E-08	2.33E-06
GO:0001944	Vasculature Development	BP 4	532	18 (3.4%)	7.25E-08	2.93E-06
GO:0010038	Response to Metal Ion	BP 4	177	11 (6.2%)	7.81E-08	2.93E-06
GO:2000026	Regulation of Multicellular Organismal Development	BP 4	1180	27 (2.3%)	1.10E-07	3.81E-06
GO:0060537	Muscle Tissue Development	BP 4	377	15 (4.0%)	1.32E-07	4.23E-06
GO:0070848	Response to Growth Factor Stimulus	BP 4	331	14 (4.3%)	1.56E-07	4.69E-06
GO:0070997	Neuron Death	BP 4	194	11 (5.7%)	1.99E-07	5.35E-06
GO:0042692	Muscle Cell Differentiation	BP 4	336	14 (4.2%)	2.02E-07	5.35E-06
GO:0009966	Regulation of Signal Transduction	BP 4	1752	33 (1.9%)	3.27E-07	7.41E-06
GO:0072358	Cardiovascular System Development	BP 4	791	21 (2.7%)	3.29E-07	7.41E-06
GO:0072359	Circulatory System Development	BP 4	791	21 (2.7%)	3.29E-07	7.41E-06
GO:0009889	Regulation of Biosynthetic Process	BP 4	3114	47 (1.5%)	3.83E-07	8.20E-06
GO:0060255	Regulation of Macromolecule Metabolic Process	BP 4	3845	53 (1.4%)	9.28E-07	1.90E-05
GO:0048545	Response to Steroid Hormone Stimulus	BP 4	232	11 (4.7%)	1.24E-06	2.43E-05
GO:0036293	Response to Decreased Oxygen Levels	BP 4	189	10 (5.3%)	1.37E-06	2.57E-05
GO:0035556	Intracellular Signal Transduction	BP 4	1710	31 (1.8%)	1.95E-06	3.51E-05
GO:0009892	Negative Regulation of Metabolic Process	BP 4	1382	27 (2.0%)	2.27E-06	3.94E-05
GO:0051094	Positive Regulation of Developmental Process	BP 4	694	18 (2.6%)	3.40E-06	5.67E-05
GO:0014070	Response to Organic Cyclic Compound	BP 4	498	15 (3.0%)	4.00E-06	6.42E-05
GO:0033993	Response to Lipid	BP 4	502	15 (3.0%)	4.30E-06	6.67E-05
GO:0097190	Apoptotic Signaling Pathway	BP 4	442	14 (3.2%)	4.78E-06	7.09E-05
GO:0009743	Response to Carbohydrate Stimulus	BP 4	129	8 (6.2%)	4.93E-06	7.09E-05
GO:0080090	Regulation of Primary Metabolic Process	BP 4	3945	52 (1.3%)	5.04E-06	7.09E-05

Biological Process enriched in FOXO TFs target genes using Gene Ontology.

Online Table VI

Echocardiographic parameters at 4 weeks of age in the experimental groups

	WT	***Lmna*$^{-/-}$**	***Lmna*$^{-/-}$*:AAV9-Gfp***	***Lmna*$^{-/-}$:AAV9-FOXO^{shRNA}**	**ANOVA**
N	18	12	9	16	
M/F	7/11	6/6	3/6	9/7	
Age (days)	28.2±2.1	28.4±1.9	28.5±1.1	29.4±11	0.19
Body weight (g)	14.1±3.7	7.95±1.8***	9.99±1.3 §§	9.7±2.2‡‡‡	<0.0001
HR (bpm)	524±72	514±68	565±66	550±97	0.37
IVST (mm)	0.59±0.049	0.54±0.063	0.59±0.055	0.52±0.044‡‡, ##	0.0004
PWT (mm)	0.60±0.1	0.54±0.06	0.55±0.07	0.48±0.07‡‡	0.0018
LVEDD (mm)	3.27±0.3	2.82±0.47	3.54±0.41§§	3.44±0.61‖‖	0.0021
LVEDDi (mm/g)	0.24±0.05	0.36±0.04***	0.36±0.05†††,§§	0.36±0.05‡‡‡	<0.0001
LVESD (mm)	1.57±0.26	1.86±0.58	2.7±0.63†††,§	2.63±0.86‡‡‡,‖‖	<0.0001
LVESDi (mm/g)	0.244±0.05	0.36±0.04***	0.36±0.05†††	0.36±0.05‡‡‡	<0.0001
FS (%)	52.17±6.64	35.12±8.36***	24.56±9.45§§§	25.31±12.86‡‡‡	<0.0001
LVM (mg)	54.62±12.47	37.81±14.37**	58.48±11.47§§	47.28±12.95	0.0016
LVMi (mg/g)	3.99±0.89	4.67±0.71	5.82±0.68†††,§	4.94±0.88‡‡	<0.0001

Abbreviations: As in Table II

*:$p \leq 0.05$, **: $p \leq 0.01$, ***: $p \leq 0.001$ for *Lmna*$^{-/-}$ *vs* WT.
† $p \leq 0.05$, ††: $p \leq 0.01$, †††: $p \leq 0.001$ for *Lmna*$^{-/-}$:GFP *vs* WT.
‡:$p \leq 0.05$, ‡‡: $p \leq 0.01$, ‡‡‡: $p \leq 0.001$ for *Lmna*$^{-/-}$:FOXO^{shRNA} *vs* WT.

§:$p \leq 0.05$, §§: $p \leq 0.01$, §§§: $p \leq 0.001$ for *Lmna*$^{-/-}$:GFP *vs Lmna*$^{-/-}$.
‖:$p \leq 0.05$, ‖‖: $p \leq 0.01$, ‖‖‖: $p \leq 0.001$ for *Lmna*$^{-/-}$:FOXO^{shRNA} *vs Lmna*$^{-/-}$.

#:$p \leq 0.05$, ##: $p \leq 0.01$, ###: $p \leq 0.001$ for *Lmna*$^{-/-}$:FOXO^{shRNA} *vs Lmna*$^{-/-}$:GFP.

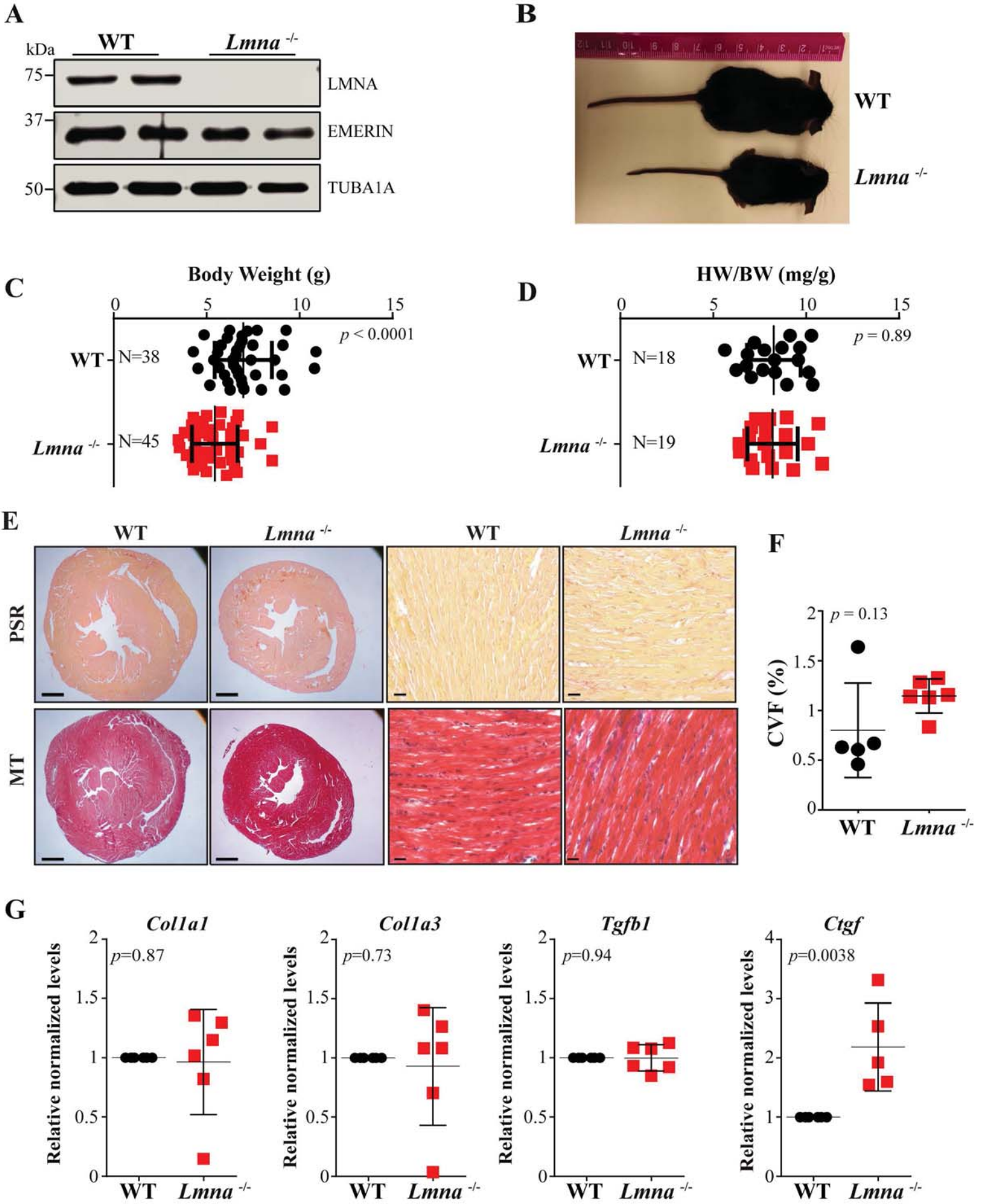

Online Figure I: Phenotype of the *Lmna*$^{-/-}$ mice at 2 weeks of age, the time point used for RNA-Sequencing.
A. Immunoblot showing absence of the LMNA protein in the *Lmna*$^{-/-}$ mice. Emerin and tubulin α1 (TUBA1A) as controls. **B.** Gross morphology **C.** Body weight. **D.** HW/BW ratio. **E.** Representative low and high magnification myocardial sections stained for Picro-Sirius Red (PSR) and Masson's trichrome (MT) showing absence of intrestitial fibrosis. Scale bar is Bar is 200 μm in left panels and 20 μm in right panels **F.** Collagen volume fraction (CVF). **G.** Transcript levels of selected genes invovled in fibrosis: collagen, type Iα1 (*Col1a1*), collagen, type IIIα1 (*Col3a1*), transforming growth factor *β*1 (*Tgfβ1*), and connective tissue growth factor (*Ctgf*), as determined by qRT-PCR.

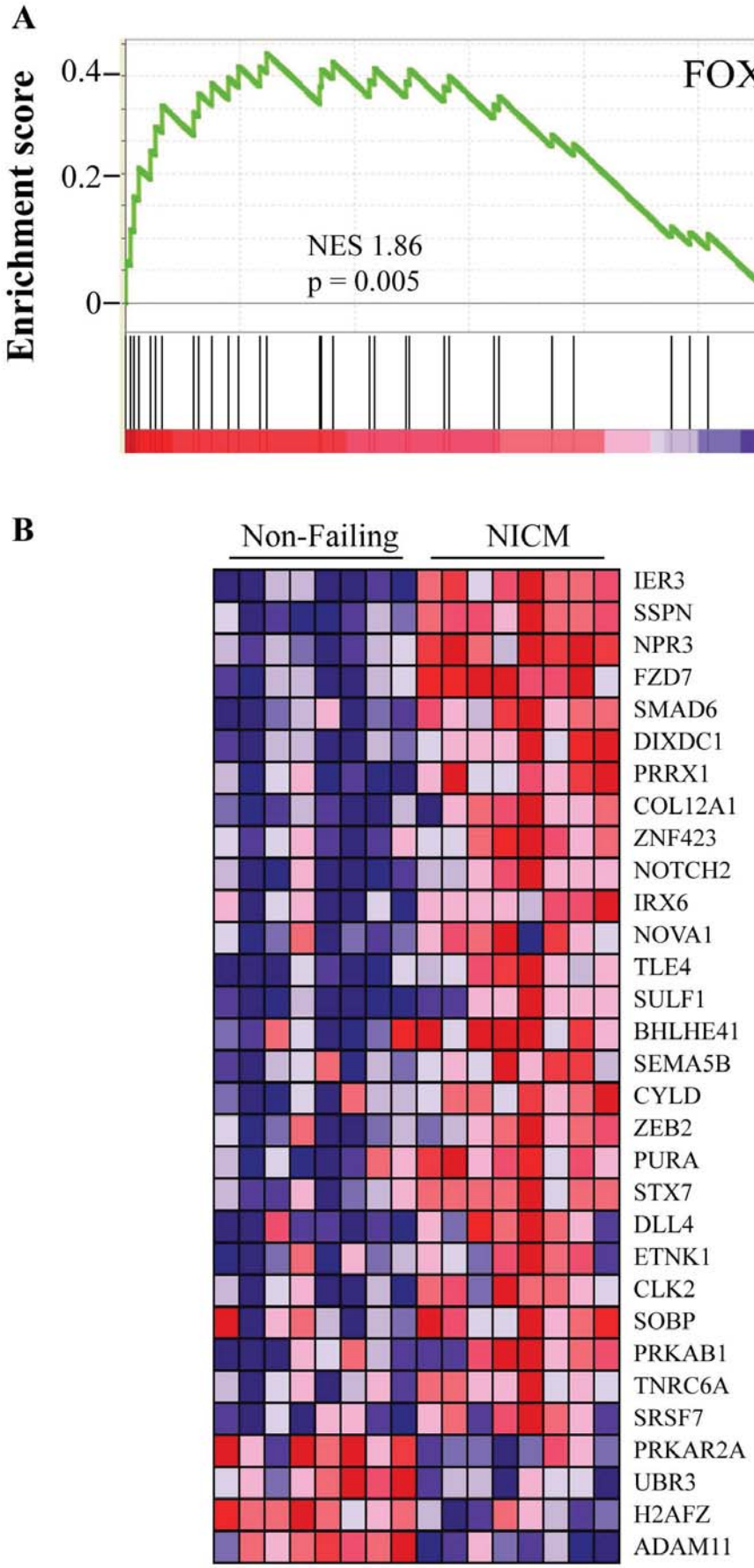

Online Figure II: Differenitally expressed transcripts of FOXO TF tagets in human dilated cardiomyopathy with undefined mutation.

GSEA analysis for transcription factor motif enrichment of Human RNA-seq data (GSE46224) obtained from left ventricular tissues of adult non-failing and non-ischemic cardiomyopathy (NICM) hearts with undefined causal mutations.

A. GSEA enrichment plot of FOXO transcription factors, which were identified by the enrichment of their canonical binding site (TTGTTT_V$FOXO4_01). The motif was among the top 10 enriched TF motifs.

B. Heat map showing FOXO TF target transcripts that indicate activation of FOXO TF in the GSEA analysis.

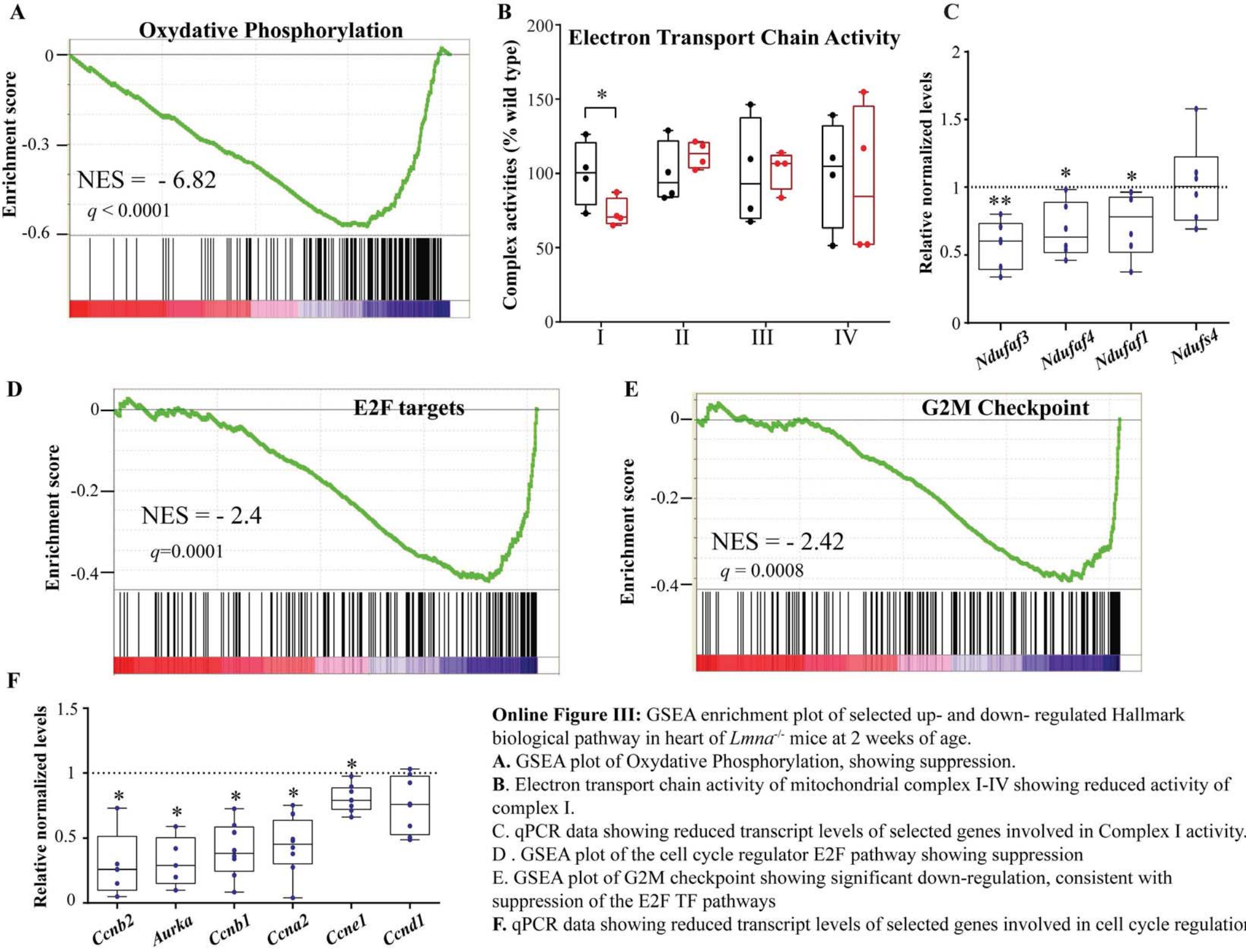

Online Figure III: GSEA enrichment plot of selected up- and down- regulated Hallmark biological pathway in heart of *Lmna*$^{-/-}$ mice at 2 weeks of age.

A. GSEA plot of Oxydative Phosphorylation, showing suppression.

B. Electron transport chain activity of mitochondrial complex I-IV showing reduced activity of complex I.

C. qPCR data showing reduced transcript levels of selected genes involved in Complex I activity.

D . GSEA plot of the cell cycle regulator E2F pathway showing suppression

E. GSEA plot of G2M checkpoint showing significant down-regulation, consistent with suppression of the E2F TF pathways

F. qPCR data showing reduced transcript levels of selected genes involved in cell cycle regulation

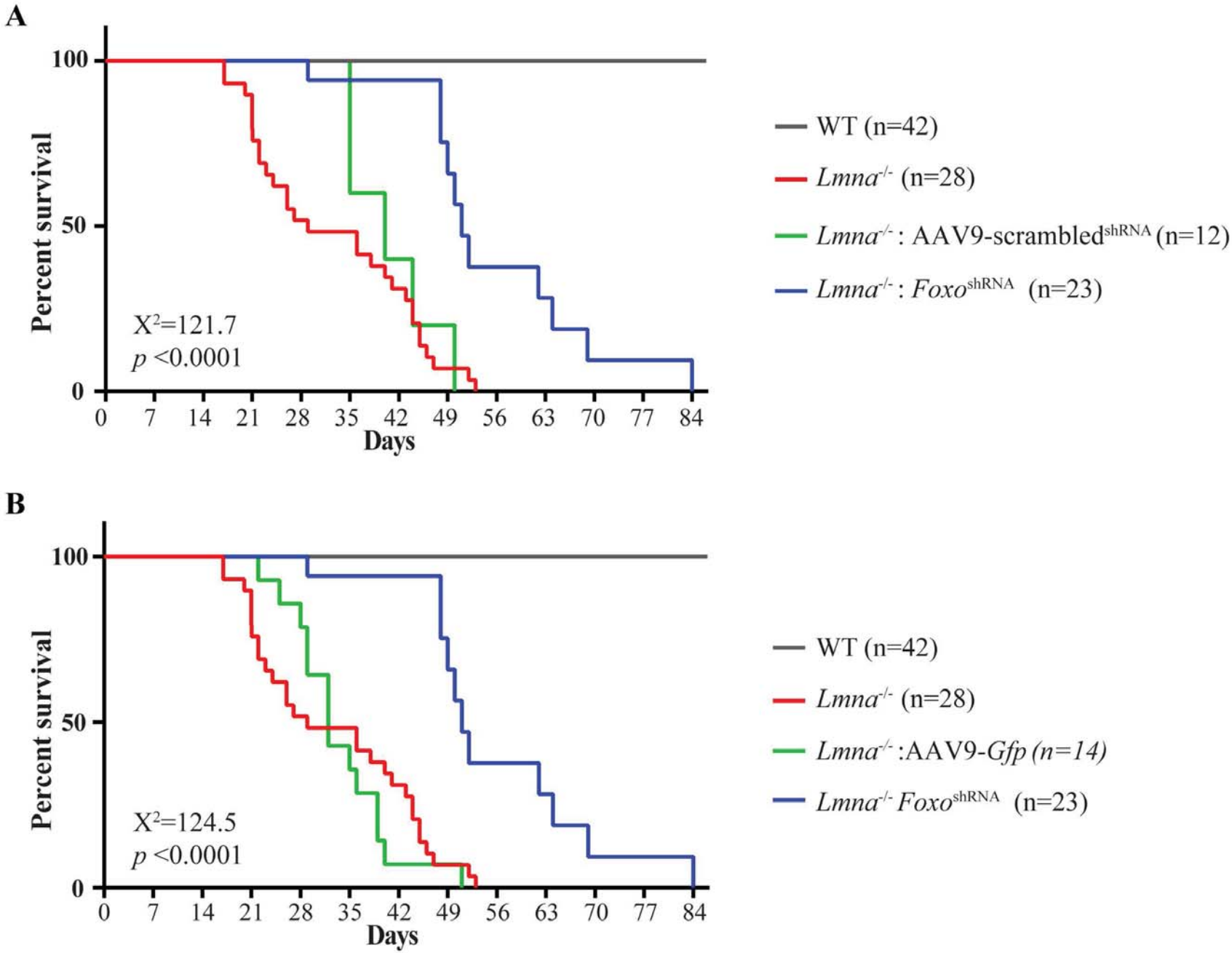

Figure IV: Kaplan-Meier survival plots of wild type (WT), *Lmna*$^{-/-}$ mice (not injected) and *Lmna*$^{-/-}$ mice injected either with a AAV9-scrambled^{shRNA} (Panel A) or AAV9:*Gfp* (Panel B) constructs as two separate controls or with the AAV9-*Foxo*^{shRNA} construct. Survival improved in the AAV9-*Foxo*^{shRNA} in both experiments as compared to control viruses or not injected *Lmna*$^{-/-}$ mice.

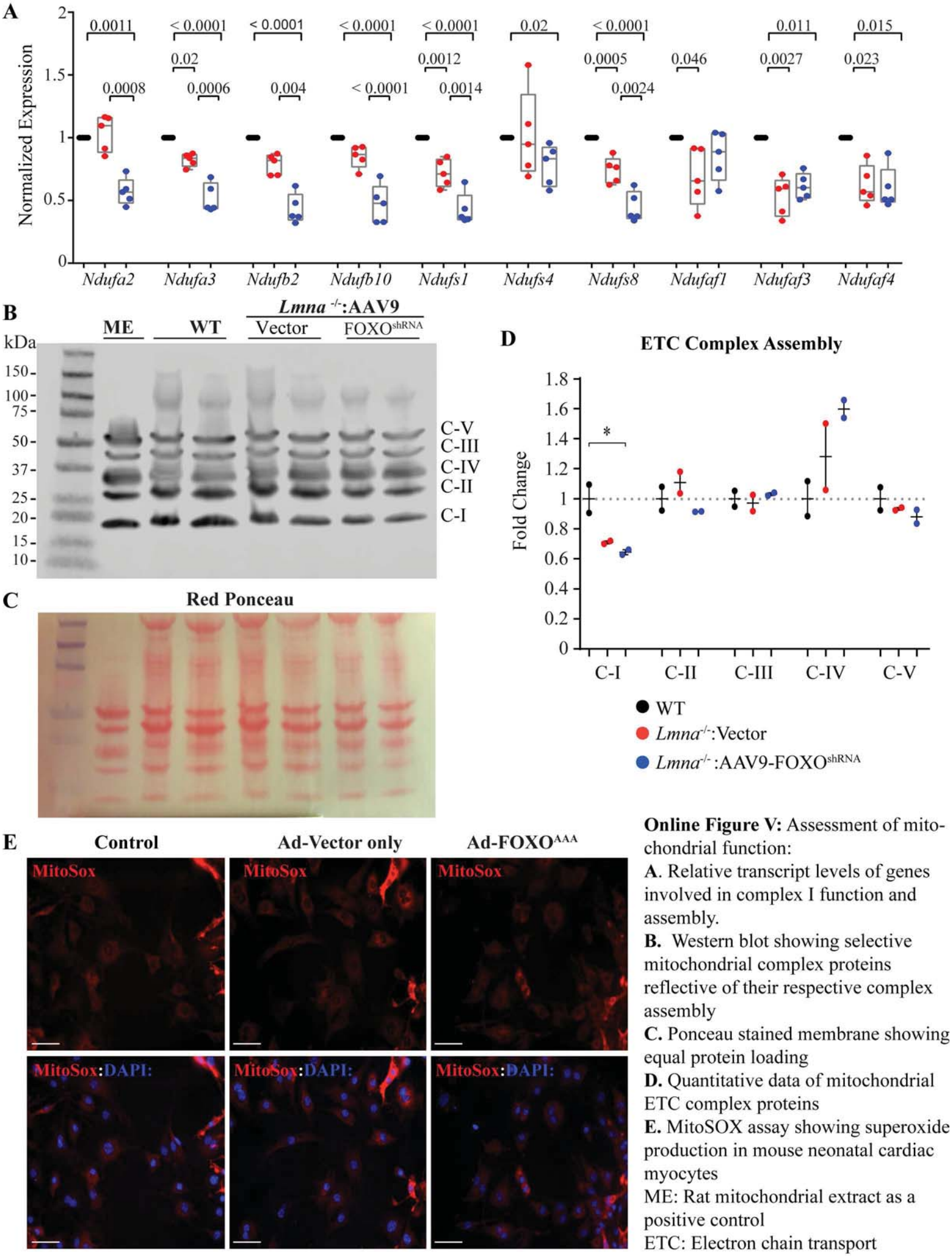

Online Figure V: Assessment of mitochondrial function:

A. Relative transcript levels of genes involved in complex I function and assembly.

B. Western blot showing selective mitochondrial complex proteins reflective of their respective complex assembly

C. Ponceau stained membrane showing equal protein loading

D. Quantitative data of mitochondrial ETC complex proteins

E. MitoSOX assay showing superoxide production in mouse neonatal cardiac myocytes

ME: Rat mitochondrial extract as a positive control

ETC: Electron chain transport

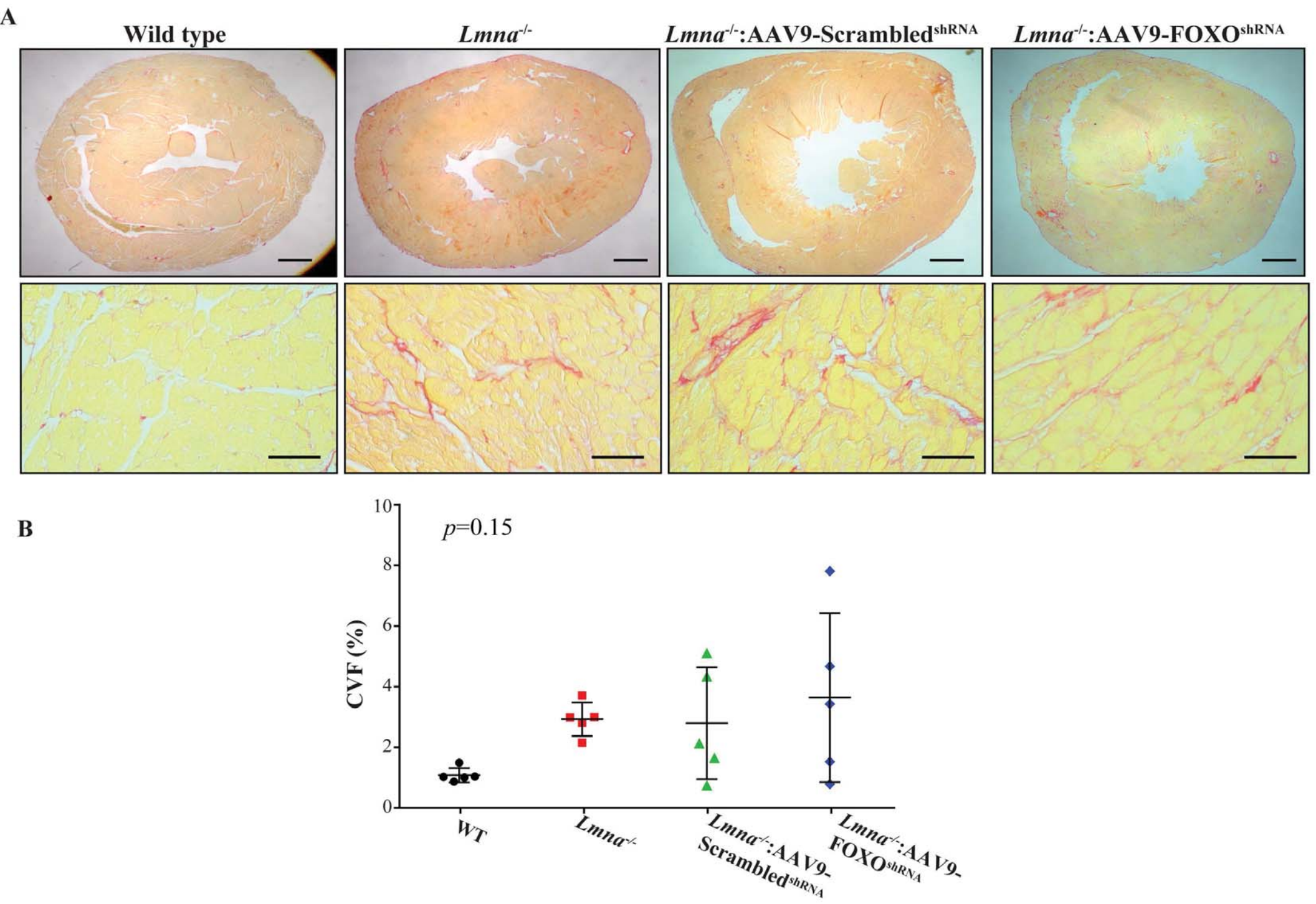

Online Fiigure VI: Interstitial fibrosis in the wild type, *Lmna*$^{-/-}$, *Lmna*$^{-/-}$ treated with AAV9-Scrambled^{shRNA} and *Lmna*$^{-/-}$ treated with AAV9-FOXO^{shRNA} **A.** Low (x2) and high (X40) magnification fields of picro sirius red stained thin myocardial sections in the experimental groups. Scale bar is 200μm and 20μm. **B.** Quantitative collagen volume fraction (CVF) as percent of the myocadium in the experimental groups.

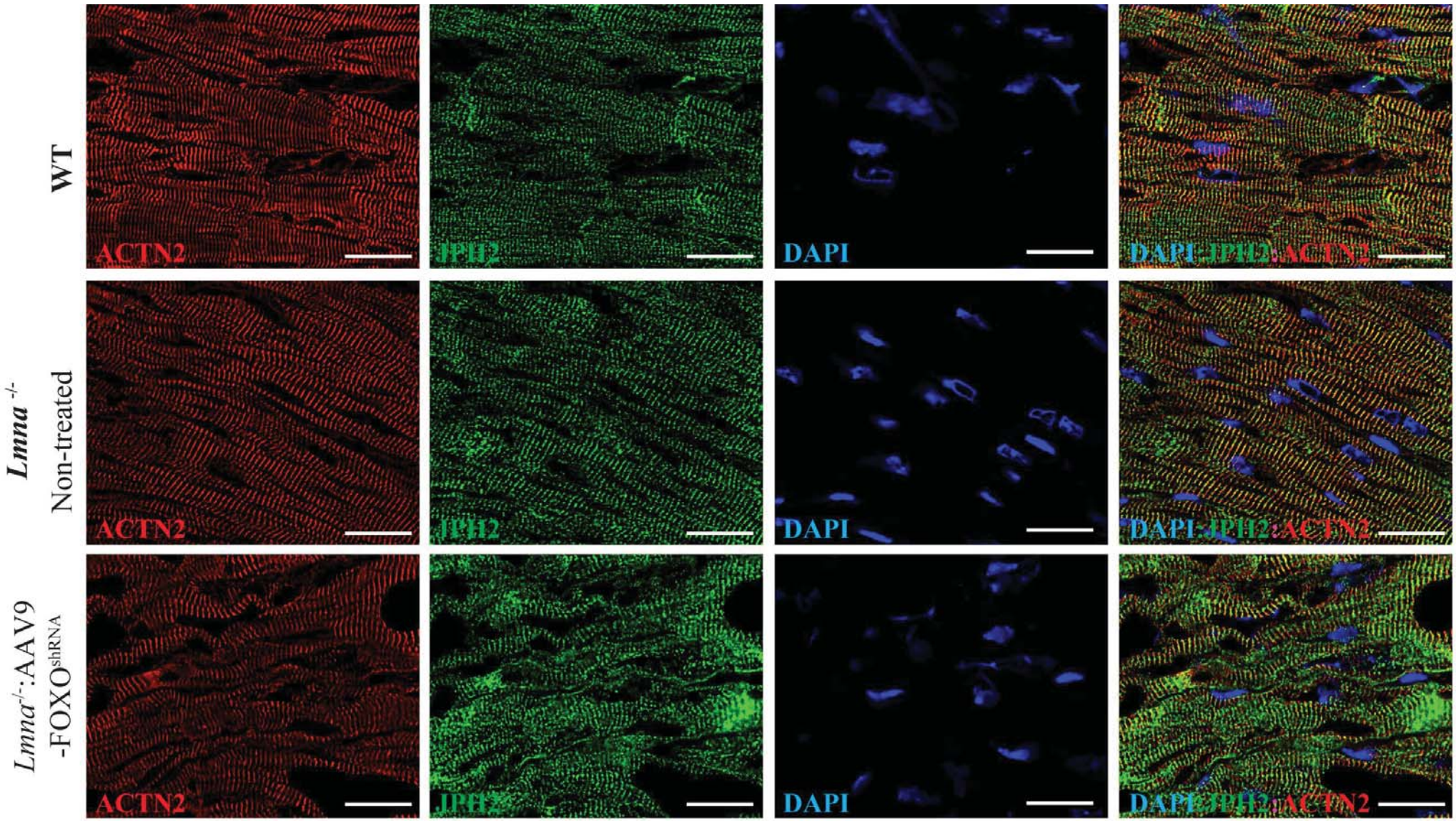

Online Figure VII. Myocardial structure
Immunofluorescence staining of thin myocardial sections for actinin alpha 2 (ACTN2), and junctophilin 2 (JPH2) in wild type (WT), Lmna-/- mice and $Lmna^{-/-}$ mice treated with an AAV9 construct expressing an shRNA against FOXO transcription factors ($Lmna^{-/-}$:AAV9-$FOXO^{shRNA}$)